Struct Multidisc Optim (2013) 48:747–762
DOI 10.1007/s00158-013-0924-7

RESEARCH PAPER

An optimization-based method for designing modular systems that traverse dynamic s-Pareto frontiers

P. K. Lewis · C. A. Mattson

Received: 17 October 2012 / Revised: 4 February 2013 / Accepted: 7 March 2013 / Published online: 21 April 2013

Abstract The use of multiobjective optimization in identifying systems that account for changes in needs (preferences), operating environments, concepts, and analysis models over time is generally not explored. In terms of identifying sets of non-dominated designs, these changes result in the concept of *dynamic Pareto frontiers*, or *dynamic s-Pareto frontiers* in cases where *sets* of system concepts are being evaluated simultaneously over time. In a previous work by the authors, a 6-step optimization-based method was presented to identify systems that account for predicted changes in preferences by moving from one s-Pareto design to another through module addition. Addressing some of the limitations of this method, this paper presents an improved 5-step optimization-based method that builds on recent developments in multiobjective problem formulations of dynamic s-Pareto frontiers. In addition, recognizing the inherent uncertainty associated with predicting future needs or preferences and dynamic s-Pareto frontiers, the incorporation of uncertainty analysis in this improved method is also presented as an additional method improvement. Application of the presented method is illustrated through a modular plywood cart system for developing countries.

Keywords Dynamic s-Pareto frontiers · Multiobjective optimization · Modular system design · Pareto traversing

P. K. Lewis · C. A. Mattson (✉)
Department of Mechanical Engineering,
Brigham Young University, Provo, UT 84602, USA
e-mail: mattson@byu.edu

Nomenclature

J	Aggregate objective function.
μ	Vector of design objectives.
x	Vector of design objects.
y	Vector of independent design objects.
z	Vector of dependent design objects.

Subscripts, superscripts, and other indicators

$[\ ]^{(i)}$	indicates current module.
$[\ ]^{(k)}$	indicates current design concept.
$n_{[\ ]}$	indicates the number of [ ].
$[\ ]_{l/u}$	indicates the lower/upper limit of [ ].
$\hat{[\ ]}$	indicates the modular-system [ ].
$[\ ]^*$	indicates the optimal value of [ ].

1 Introduction & background

Engineering design is a multifaceted decision making process that often involves several conflicting design objectives (Das 1999; Kasprzak and Lewis 2000; Frischknecht et al. 2011). The use of multiobjective optimization in resolving conflicts due to changes in needs (preferences), operating environments, concepts, and analysis models over time is generally not explored. When identifying sets of non-dominated designs, these changes result in the concept of *dynamic Pareto frontiers*, or *dynamic s-Pareto frontiers* in cases where *sets* of system concepts (Mattson and Messac 2003) are being evaluated simultaneously over time (Lewis et al. 2012).

The concept of changing design selection due to changes in preference, analysis models, concepts, or environment is illustrated is Fig. 1 where the points $\mu^{(1)}$, $\mu^{(2)}$, and $\mu^{(3)}$ represent the designs selected along the dynamic

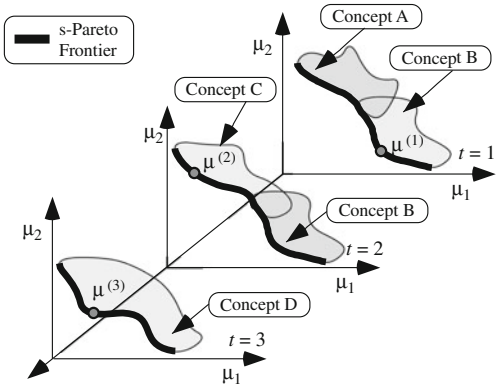

Fig. 1 Design selections due to both changing preference and dynamic s-Pareto frontiers

Pareto/s-Pareto frontier (bold lines) at times 1, 2, and 3 respectively. As identified in Lewis et al. (2012), some examples of situations where these changes could be predicted include changes in manufacturing cost models due to economies of scale, planned implementation of new technologies, ranges of known operating environments, and governmental performance regulation changes (i.e., gas mileage or emission requirements of vehicles).

The decision of whether to account for these changes through the development of multiple systems, or adaptive/reconfigurable/modular systems is a complex decision. In a previous work by the authors, a six-step optimization-based method was presented to identify a catalog/series of system designs that account for predicted changes in preferences by moving from one s-Pareto design to another through module addition (Lewis and Mattson 2012). Addressing some of the limitations of this method, this work presents an improved 5-step optimization-based method that builds on recent developments in multiobjective problem formulations of dynamic s-Pareto frontiers (Lewis et al. 2012).

To lay the foundation for this improved method, a summary of the original six-step method is provided in Section 2, followed by the presentation of the improved method in Section 3. Identification of a modular cart system for developing countries is then provided in Section 4 to illustrate the implementation of the improved method, with conclusions provided in Section 5.

2 Summary of the original six-step optimization-based method

A Pareto/s-Pareto frontier, by nature, represents all optimal system candidates (Messac and Mattson 2004; Todoroki and Sekishiro 2008; Gurnani and Lewis 2008). As such, one of the fundamental tenets of this method is that the current and future needs of a system can be represented by individual

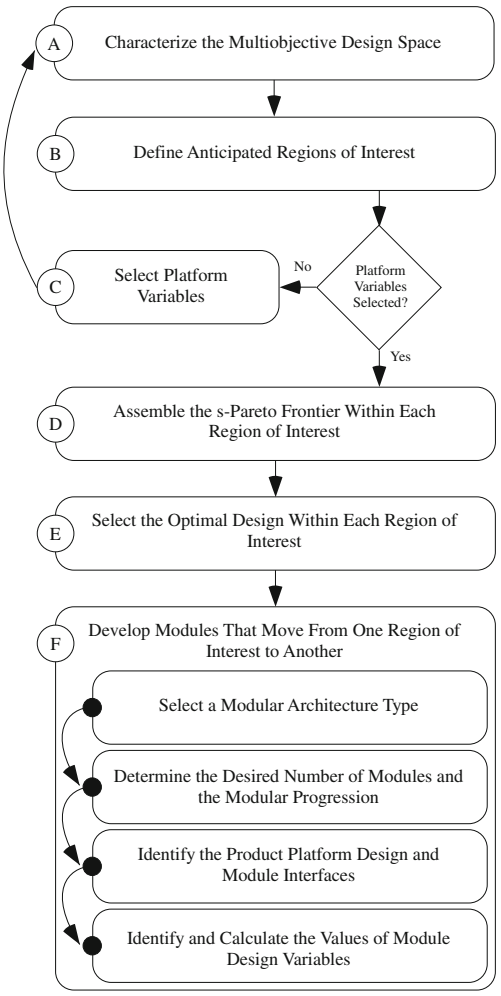

Fig. 2 Flow chart describing the six-step optimization-based modular-system design method presented in Lewis and Mattson (2012)

designs along the s-Pareto frontier. Building on this assumption, the novel outcome of this method (see Fig. 2) is that it identifies designs along the s-Pareto frontier that facilitate the creation of modules that jump from one location on the frontier to another. These non-dominated designs are selected based on models of present and future needs, and are used to provide target performance values in the design of platforms and modules. This concept is graphically represented for a s-Pareto design situation in Fig. 3. The designs represented by $\mu^{(1)}$–$\mu^{(4)}$ represent the designs satisfying the present/future needs that define the boundaries of a set of anticipated regions of interest. The identified platform and modules are subsequently designed to achieve the desired system performances identified by the designs $\mu^{(1)}$–$\mu^{(4)}$.

2.1 Summary of steps

This method of using models of present and future needs to guide the design of a modular-system using target s-Pareto

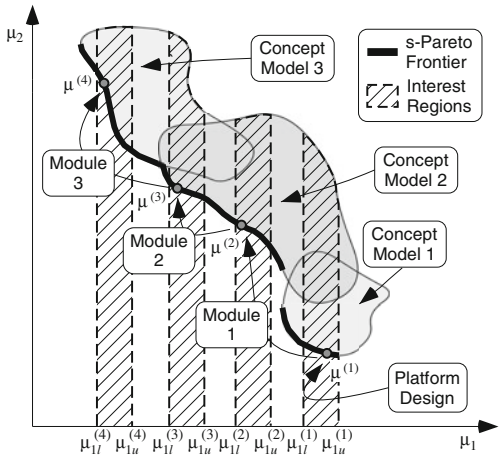

Fig. 3 Graphical representation of the intent/result of the method presented in Fig. 2. Notice that the identified modular-system can adapt to designs that are within designer defined regions of interest representing the current and future system needs

designs is an iterative six-step process. Each of these steps, as presented in Lewis and Mattson (2012), is summarized below.

Step A: Explore the multiobjective design space of each system concept to identify the Pareto frontier for each of the selected system concepts.

Step B: Identify *Anticipated Regions of Interest* within the multiobjective design space that capture the predicted changes in customer needs over time.

Step C: Identify platform design variables (x_p) that minimize the losses in objective space performance due to the added constraint of commonality within the anticipated regions of interest.

Step D: Identify the s-Pareto frontier within each region of interest.

Step E: Identify a single *s-Pareto*-optimal design within each region of interest that facilitates the desired adaptation to designs selected in the other regions of interest. The multiobjective problem formulations capable of identifying the optimal design in each region of interest for Pareto and s-Pareto settings are not repeated here, but are provided in Lewis and Mattson (2012).

Step F: Identify module designs that provide a constrained change in system performance by: (i) Selecting a modular architecture type, (ii) Identifying the product platform design and module interfaces, (iii) Determining the desired number of modules and modular progression, and (iv) Identifying and calculating the values of module design variables through a constrained module optimization formulation. Once again, the formulations required to complete this step are not repeated here. The developed formulation for constrained-module optimization are also presented in Lewis and Mattson (2012).

It should be noted that the development of this method was divided into two phases. The first phase focused on the development of systems capable of traversing a single Pareto frontier, while the second phase extended the method to s-Pareto design situations. For complete presentations of these phases of method developments, see Lewis et al. (2011) and Lewis and Mattson (2012) respectively.

2.2 Original method limitations

The purpose of this section is to describe the limitations of the six-step method that provide the motivation for the method presented in Section 3. Specifically, the notable limitations of this method include the following:

(i) The method is only capable of accounting for changes in preferences and environment. The multiobjective problem formulation implemented in Step E of the method cannot identify a dynamic s-Pareto frontier if different sets of concepts or analysis models need to be considered within each region of interest (i.e., considered concepts and analysis models cannot change over time).

(ii) The method assumes that a common set of design variables can be identified as platform variables (excludes the possibility of considering totally different concepts). This requirement of only considering concepts that collectively contain a set of common variables predefines the optimization results, and does not allow for concepts with potential improvements in objective space performance to influence the modular-system concepts that are developed.

(iii) The optimization of each module is performed separate from the other elements of the modular-system, and assumes that the platform and specified module combinations achieve the desired performance. Consequently, the constrained module optimization formulation in Step F does not account for the possibility that the performance of system iterations achieved through the addition of specific modules do not match the target performances identified in Step E of the method.

(iv) Due to the use of predicted changes in preferences and environments, along with the desire to allow changes in analysis models and concepts, uncertainty is an inherent issue that is not incorporated or discussed in the current optimization formulations.

In considering the anticipated sources of uncertainty, three general groups that emerge are *parameter/variable uncertainty*, *analysis model output uncertainty*, and *current/future preference uncertainty*. In the literature are found two broad categories of approaches to determining the level of uncertainty in decision making. The first are *reliability-based design methods* (Frangopol and Corotis 1996; Thanedar and Kodiyalam 1991; Melchers 1999) which focus on assessing the probability of design failure, and seek to reduce such probabilities by shifting the mean performance away from constraint limits (Melchers 1999). The second are *robust design based methods* (Parkinson et al. 1995; Chen et al. 1999; Chen et al. 2000; Su and Renaud 1997; Taguchi 1993; Messac and Ismail-Yahaya 2002; Chen and Wassenaar 2001) which focus on optimizing the mean performance, and minimizing performance variation, while maintaining feasibility with probabilistic constraints (Taguchi 1993; DeVor et al. 1992; Koch 2002). Note that these two approaches have generally focused on parameter/variable and model output uncertainty. As such, the incorporation of uncertainty mitigation into the method presented in Section 3 will focus on accounting for current/future preference uncertainty.

Some of the common methods of performing uncertainty analysis include: (i) Monte Carlo and Sampling techniques (Halton 1960; Hammersley 1960; Owen 1998; Hutcheson and McAdams 2010), (ii) Univariate Dimension Reduction (Xiong et al. 2011; Li and Zhang 2011), (iii) Deterministic Error by Model Composition (Larson et al. 2010), (iv) Error Budgets (Evans et al. 2009; Hamaker 1995), (v) Interval Analysis Methods (Hayes 2003), (vi) Bayesian Inference (Box and Tiao 1992), (vii) Anti-Optimization Techniques (Lombardi and Haftka 1998; Gurav et al. 2005), and (viii) Taylor Series and Central Moments (Koch 2002; Glancy 1999; Vardeman 1994; Jackson 1982). Note that the analysis of multiple predicted design scenarios inherent in the presented method will often decrease the likelihood of being able to obtain statistical data of the parameters/variables and analysis model outputs for each concept/scenario. As such, to enable the use of either statistical or bounded uncertainty parameter domains, and ensure that designs are selected such that the wost case scenarios will satisfy all design constraints, the optimization formulations within the improved method will incorporate Anti-Optimization techniques.

3 Introduction of a new 5-step modular-system optimization-based method using dynamic s-Pareto frontiers

This section presents an optimization-based method that builds on recent developments in multiobjective problem formulations of dynamic s-Pareto frontiers, and addresses the identified limitations of the method summarized in the previous section. Figure 4 illustrates the intent of the method to select an s-Pareto optimal platform design that, through the addition of modules, becomes other designs within anticipated regions of interest along the *dynamic s-Pareto frontier*. For example, the figure shows that the platform design, labeled $\mu^{(1)}$, adapts to become $\mu^{(2)}$ through the addition of Module 1. In like manner, the subsequent design identified as $\mu^{(3)}$ is also achieved through the addition of Module 2.

Figure 5 provides a flow chart that represents the five primary steps of the multiobjective optimization design method developed herein. Each of these steps is described below. It is important to note that the titles of some of the steps are similar to the steps/sub-steps of the original method presented in Fig. 2. However, each of these steps requires new and essential extensions to enable the method to identify systems capable of traversing a dynamic s-Pareto frontier.

3.1 Characterize the dynamic multiobjective design space

The first step of the method is to explore the dynamic multiobjective design space to obtain information that will help to guide and inform the development of modular system concepts in the fourth step of the method (see Section 3.4). As seen in Fig. 4, this requires the characterization of the dynamic s-Pareto frontier for the set of *non-modular* system concepts that account for the identified changes in preferences, concepts, models, and environments over time. As such, the expanded function of this step of the method requires the evaluation of a Dynamic s-Pareto Optimization Formulation as presented in Lewis et al. (2012), where a noted capability of this formulation

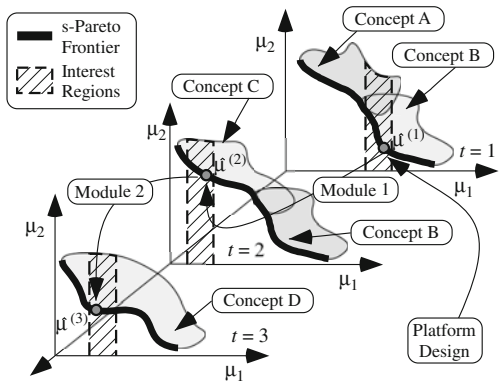

Fig. 4 Graphical representation of the intent of the improved method to provide a system that expands from one *dynamic s-Pareto design* to another through the addition of modules. Also notice that the designs that it can adapt to are within designer defined regions of interest

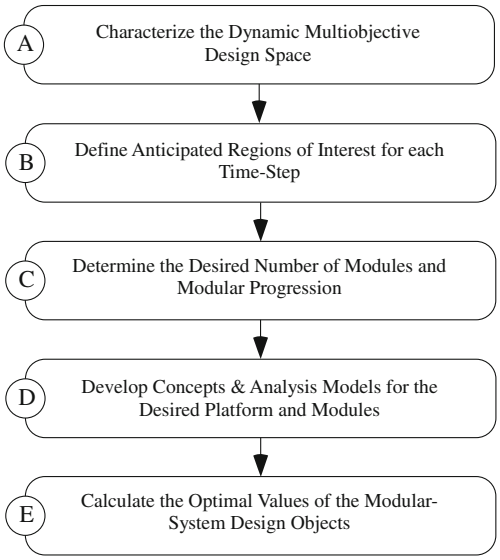

Fig. 5 Flow chart describing the five-step multiobjective optimization design method developed in this section

is that it does not require the identification of common design elements (i.e., considered concepts can be totally different). It should be noted that this dynamic formulation enables design variables, models, concepts, and constraints to change seamlessly. As a result, as MOP formulations change, what was a design parameter in one formulation could be an inequality constraint in the next formulation. Thus, to avoid confusion, any variable, parameter, constraint, or objective associated with a design is termed a *design object*.

As described in the previous section, there also exists the need to incorporate uncertainty analysis into the method presented in this section. With this understanding, a generic dynamic multiobjective optimization problem capable of identifying the s-Pareto frontier for each time step (Lewis et al. 2012), and incorporating anti-optimization is presented as *Problem 1* (*P1*):

$$\min_{k^{(t)}} \left\{ \min_{y^{(k^{(t)})}} \left\{ \mu_1^{(k^{(t)})}\left(x^{(k^{(t)})}\right), \ \ldots, \ \mu_{n_\mu^{(k^{(t)})}}^{(k^{(t)})}\left(x^{(k^{(t)})}\right) \right\} \left(n_\mu^{(k^{(t)})} \geq 2\right) \right\} \left\{k = 1, \ldots, n_k^{(t)}\right\} \tag{1}$$

subject to:

$$y_{l,i}^{(k^{(t)})} \leq y_i^{(k^{(t)})} \leq y_{u,i}^{(k^{(t)})} \quad \left\{i = 1, \ldots, n_y^{(k^{(t)})}\right\} \tag{2}$$

$$g_{\max,j}^{(k^{(t)})} \leq 0 \quad \left\{j = 1, \ldots, 2n_z^{(k^{(t)})}\right\} \tag{3}$$

where:

$$\mu^{(k^{(t)})} = w^{(k^{(t)})} \cdot x^{(k^{(t)})} \tag{4}$$

$$w^{(k^{(t)})} = \begin{bmatrix} w_{1,1}^{(k^{(t)})} & \cdots & 0 \\ \vdots & \ddots & \vdots \\ 0 & \cdots & w_{n_x^{(k^{(t)})},n_x^{(k^{(t)})}}^{(k^{(t)})} \end{bmatrix} \tag{5}$$

$$x^{(k^{(t)})} = \left[y_1^{(k^{(t)})}, \ldots, y_{n_y^{(k^{(t)})}}^{(k^{(t)})}, z_1^{(k^{(t)})}\left(y^{(k^{(t)})}\right), \ldots, z_{n_z^{(k^{(t)})}}^{(k^{(t)})}\left(y^{(k^{(t)})}\right) \right]^T \tag{6}$$

$$n_x^{(k^{(t)})} = n_y^{(k^{(t)})} + n_z^{(k^{(t)})} \tag{7}$$

where $x^{(t)}$ is a vector composed of independent $\left(y^{(k^{(t)})}\right)$ and dependent $\left(z^{(k^{(t)})}\right)$ design objects at time step t; and the objectives identifier matrix $\left(w^{(k^{(t)})}\right)$ is a diagonal matrix for time step t satisfying the condition $w_{i,i}^{(k^{(t)})} = \{-1, 0, 1\}$; Note that $\mu_i^{(k^{(t)})}$ will be maximized or minimized for values of $w_{i,i}^{(k^{(t)})} = -1$ and $w_{i,i}^{(k^{(t)})} = 1$ respectively. In addition, the values of $g_{\max,j}^{(k^{(t)})}$ come from the following anti-optimization:

$$\max_{c^{(k^{(t)})}} \left\{ g_j^{(k^{(t)})}\left(y^{(k^{(t)})}, c^{(k^{(t)})}\right) \right\} \tag{8}$$

subject to:

$$h_v^{(k^{(t)})}\left(c^{(k^{(t)})}\right) \leq 0 \quad \left\{v = 1, \ldots, n_h^{(k^{(t)})}\right\} \tag{9}$$

where:

$$g_j^{(k^{(t)})} = \begin{cases} z_j^{(k^{(t)})}\left(y^{(k^{(t)})}, c^{(k^{(t)})}\right) - z_{u,j}^{(k^{(t)})} & , j \leq n_z^{(k^{(t)})} \\ -z_{j-n_z^{(k^{(t)})}}^{(k^{(t)})}\left(y^{(k^{(t)})}, c^{(k^{(t)})}\right) + z_{l,j-n_z^{(k^{(t)})}}^{(k^{(t)})} & , \text{else} \end{cases} \tag{10}$$

where $c^{(k^{(t)})}$ which reside in the domain defined by (9). Note that for discrete representations of the s-Pareto frontier at each time step, the corresponding $x^{*(k^{(t)})}$ vector and corresponding $k^{(t)}$ for each discrete point are collected in the sets D_{x} and D_{k}. The mathematical definitions of these sets are: $D_{\mathrm{x}} := \left\{ \left(x_1^{*(t)}, \ldots, x_{n_p^{(t)}}^{*(t)} \right) | \forall t \in (1, 2, \ldots, n_t) \right\}$ and $D_{\mathrm{k}} := \left\{ \left(k_1^{*(t)}, \ldots, k_{n_p^{(t)}}^{*(t)} \right) | \forall t \in (1, 2, \ldots, n_t) \right\}$, where $n_p^{(t)}$ is the number of discrete s-Pareto points identified for the t-th time-step.

3.2 Define anticipated regions of interest for each time-step

As with the method presented in Section 2 (Lewis and Mattson 2012), a key idea of the method presented in this section is that changes in the desired system performance are equivalent to changes in the desired values of one or more design objectives. To that end, the second step of the method captures the predicted changes in system needs over time, and represents them as *Anticipated Regions of Interest* of the dynamic multiobjective design space. It is important to note that these regions represent predicted future needs regarding objective performance. To maintain simplicity in the graphical presentation of Fig. 4, regions of interest involving only one objective (μ_1) are shown. However, it is expected that regions of interested would be specified for as many of the objectives as desired.

As described in Section 2.1, the identification/use of current and predicted future preferences naturally introduces uncertainty in the bounds of the regions of interest identified in this step of the method. Whether statistical data or simple uncertainty bounds are known, it is suggested that at this stage in the method the bounds of the regions of interest be set to provide the largest possible regions. As a result, the upper bounds of each region of interest will be increased and the lower bounds decreased. The mitigation of the uncertainty in the bounds of the regions of interest will be addressed in the final step of the method where the designs of the modular product iterations are selected.

Although not represented in Fig. 5, it should be observed that in some situations this step of the method may occur before the method begins. One situation where this could occur is when available products on the market have predefined the acceptable ranges of system performance that is desired. In these situations the anticipated regions of interest should be incorporated into the upper and lower design object limits ($x_u^{(k^{(t)})}$ and $x_l^{(k^{(t)})}$ respectively) implemented in the dynamic s-Pareto frontier formulation presented in *P1*. In situations where this step occurs after the evaluation of *P1*, all identified dynamic s-Pareto designs outside of the anticipated regions of interest and that do not satisfy (3) are filtered out of D_{x} and D_{k}.

3.3 Determine the desired number of modules and modular progression

The purpose of this step is to leverage the knowledge gained through the characterization of the dynamic multiobjective design space in Step A in determining the number of modules to be developed, and the desired modular progression of the system. In order to determine this progression requires that a *modular architecture type* (Strong et al. 2003; Ulrich and Eppinger 2004) enabling the desired functionality of the platform and modules as a whole and *platform design target region of interest* be identified. In general, it is assumed that the platform target region corresponds to $t = 1$. However, the constrained module optimization formulation presented and evaluated in Step E is written to enable any region of interest to be selected as the platform target region.

The target result of this step of the method is the corresponding module progression matrix (δ) defining the intended module progression sequences. The definition and expected form of δ is provided below.

$$\delta = \begin{bmatrix} \alpha_0 & \beta_0 \\ \alpha_1 & \beta_1 \\ \vdots & \vdots \\ \alpha_{n_m} & \beta_{n_m} \end{bmatrix} \tag{11}$$

where the platform target region is identified by the values of α_0 and β_0 satisfying the condition $\beta_0 = \alpha_0$; and the values of α_i and β_i ($i > 0$) respectively refer to the starting and the ending regions of interest that the i-th module is bridging (i.e., a module connecting regions of interest at times one and two in Fig. 4 would correspond to a row entry of [1 2] in δ). It is noted that for the constrained module optimization formulation presented and evaluated in Step E, it is assumed that the values of β_i corresponding to each region of interest only appear once in the second column of δ.

3.4 Develop concepts & analysis models for the desired platform and modules

In the fourth step of the method, concepts and analysis models are developed for the platform and module designs that incorporate the selected modular architecture and facilitate the desired modular progression. An important aspect of these analysis models that is essential to the final step of the method is the characterization of the change in the overall system objective space performance obtained through the addition of each module. Another important goal of this step is to identify the set of modular-system design objects ($\hat{x}$) that define the platform ($\hat{x}^{(0)}$) and i-th module ($\hat{x}^{(i)}$) designs.

3.5 Calculate the optimal values of the modular-system design objects

The fifth step of the method implements an optimization routine to identify the values of the independent modular-system design objects ($\hat{y}$). The goal of this optimization for the system performance of the combined platform and modules is two-fold. The first is to minimize the distance/offset from the dynamic s-Pareto designs within each region of interest identified in the sets D_{x} and D_{k} ($\hat{\Theta}$). The second is to minimize functions that calculate a penalty value for iterations of the product that are within areas of the

regions of interest where preference uncertainties exist ($\hat{\Lambda}$). Building on the dynamic formulation presented in Step A, the generic multiobjective optimization formulation identifying the optimal values of the modular-system design objects $\left(D_{\mathrm{m}} := \left\{\left(\hat{x}_1^{*(i)}, ..., \hat{x}_{n_x^{(i)}}^{*(i)}\right) | \forall i \in \left(0, 1, ..., n_{\mathrm{m}}\right)\right\}\right)$ is presented as *Problem 2* (*P2*):

$$\min_{\hat{y}} \left\{\hat{\Lambda}^{(i)}\left(\hat{\mu}^{(i)}, \hat{\mu}_l^{(i)}, \hat{\mu}_u^{(i)}, \hat{\mu}_{l,\mathrm{unc}}^{(i)}, \hat{\mu}_{u,\mathrm{unc}}^{(i)}\right), \hat{\Theta}^{(i)}(\hat{x}^{(i)}) \mid \forall i \in (0, 1, ..., n_{\mathrm{m}})\right\} \tag{12}$$

subject to:

$$\hat{y}_{l,q}^{(i)} \le \hat{y}_q^{(i)} \le \hat{y}_{u,q}^{(i)} \quad \left\{q = 1, ..., n_{\hat{y}}^{(i)}\right\} \tag{13}$$

$$\hat{g}_{\max,j}^{(i)} \le 0 \quad \left\{j = 1, ..., 2n_{\hat{z}}^{(i)}\right\} \tag{14}$$

where:

$$\hat{y} = \hat{y}^{(0)} \cup \hat{y}^{(1)} \cup ... \cup \hat{y}^{(n\mathrm{m})} \tag{15}$$

$$\hat{\Theta}^{(i)} = \min\left(\left|\left|\mu_v^{*(\beta)} - \hat{\mu}^{(i)}\right|\right| \forall v \in \left\{1, ..., n_{\mathrm{p}}^{(\beta)}\right\}\right) \tag{16}$$

$$\hat{\mu}^{(i)} = \hat{w}^{(i)} \cdot \hat{x}^{(i)} \tag{17}$$

$$\hat{w}^{(i)} = \begin{bmatrix} \hat{w}_{1,1}^{(i)} & \cdots & 0 \\ \vdots & \ddots & \vdots \\ 0 & \cdots & \hat{w}_{n_{\hat{x}}^{(i)}, n_{\hat{x}}^{(i)}}^{(i)} \end{bmatrix} \tag{18}$$

$$\hat{x}^{(i)} = \left[\hat{y}_1^{(i)}, ..., \hat{y}_{n_{\hat{y}}^{(i)}}^{(i)}, \hat{z}_1^{(i)}\left(\hat{y}^{(i)}\right), ..., \hat{z}_{n_{\hat{z}}^{(i)}}^{(i)}\left(\hat{y}^{(i)}\right)\right]^T \tag{19}$$

$$n_{\hat{x}}^{(i)} = n_{\hat{y}}^{(i)} + n_{\hat{z}}^{(i)} \tag{20}$$

$$\mu_v^{*(\beta)} = \left\{w^{\left(k_v^{(\beta)}\right)} \cdot x_v^{*(\beta)}\right\} \rightarrow \hat{\mu}^{(i)} \tag{21}$$

$$\alpha = \delta_{i,1} \tag{22}$$

$$\beta = \delta_{i,2} \tag{23}$$

where the values of $\hat{g}_{\max,j}^{(i)}$ come from the following anti-optimization:

$$\max_{\hat{c}^{(i)}} \left\{\hat{g}_j^{(i)}\left(\hat{y}^{(i)}, \hat{c}^{(i)}\right)\right\} \tag{24}$$

subject to:

$$\hat{h}_v^{(i)}(\hat{c}^{(i)}) \le 0 \quad \left\{v = 1, ..., n_{\hat{h}}^{(i)}\right\} \tag{25}$$

where:

$$\hat{g}_j^{(i)} = \begin{cases} \hat{z}_j^{(i)}\left(\hat{y}^{(i)}, \hat{c}^{(i)}\right) - \hat{z}_{u,j}^{(i)} & , \ j \le n_{\hat{z}}^{(i)} \\ \hat{z}_{l,j-n_{\hat{z}}^{(i)}}^{(i)} - \hat{z}_{j-n_{\hat{z}}^{(i)}}^{(i)}\left(\hat{y}^{(i)}, \hat{c}^{(i)}\right) & , \ \text{else} \end{cases} \tag{26}$$

where $\hat{c}^{(i)}$ is a vector of the i-th modular system iteration uncertain parameters which reside in the domain defined by (25); D_{m} is the set of modular-system design object values ($\hat{x}^*$) for the platform ($i = 0$) and module ($i > 0$) designs; the vector $\hat{\mu}^{(i)}$ represents the objective space performance of the i-th system iteration; $\hat{y}^{(i)}$ represents the values of independent design objects that characterize $\hat{\mu}^{(i)}$; $\hat{\mu}_{l/u}^{(i)}$ are the upper/lower bounds that characterize $\hat{\mu}^{(i)}$; $\hat{\mu}_{l/u,\mathrm{unc}}^{(i)}$ are the upper/lower bounds within the regions of interest where the desirability of designs outside of these bounds is uncertain; $\hat{x}$ is a vector composed of independent $\left(\hat{y}^{(i)}\right)$ and dependent $\left(\hat{z}^{(i)}\right)$ design objects for the i-th system iteration; $\hat{w}^{(i)}$ is a diagonal matrix for the i-th system iteration satisfying the condition $\hat{w}_{q,q}^{(i)} = \{-1, 0, 1\}$; the vector $\mu^{*(\beta)}$ characterizes the objective space performance of the target designs within the region of interest for time-step β mapped to ($\rightarrow$) $\hat{\mu}^{(i)}$; $w^{\left(k_v^{(\beta)}\right)}$ is the diagonal matrix for concept k identified in (5) of *P1* for the v-th s-Pareto design of time-step β; and $x_v^{*(\beta)}$ is the design object vector for the v-th s-Pareto design of time-step β contained in D_{x}. Note that the i-th module transitions the system from the system iteration in time-step α to time-step β.

It should be observed that (12) will result in the identification of many modular-system candidates with varying values of $\hat{\Theta}$, $\hat{\Lambda}$, and the corresponding $\hat{\mu}$. Since the desired result of this final step of the method is typically a single modular-system, (12) will generally be replaced with an aggregate objective function similar in form to:

$$\min_{\hat{y}} \ J(\hat{\Theta}, \hat{\Lambda}, \hat{\mu}) \tag{27}$$

It should also be observed that (*P2*) does not provide a suggested form of the penalty function ($\hat{\Lambda}$) used in (12). The form of the penalty function is not provided so as to allow a suitable penalty to be determined by the designer. An example form of $\hat{\Lambda}$ is provided in the following section through the presented example implementation of the method described in this section.

4 Modular plywood cart system for developing countries

This section implements the method presented in Section 3 in the identification of a modular plywood cart system for developing countries. Background for the motivation and selection of this example is provided below, followed by the method implementation.

4.1 Motivation & background

Over the past thirty years, more than 17 million individuals have escaped extreme poverty through the use of *income-generating products* – products that have the potential to increase an individuals earning power (Fisher 2006; Polak 2005). Despite these measurable impacts, the distribution

of many income-generating products is limited due to the large initial investments that are required (∼2-3 months income), and the financial risks involved if the product fails to produce additional income (Fisher 2006; Johnson et al. 2006; World Resources Institute and International Finance Corporation 2007). One method to overcome these financial risks, and increase the use and distribution of these products, is through the creation of low cost modular products. One notable advantage of this approach is that the income generated by using the initial product iteration (platform iteration) serves to finance future upgrades that are made affordable through use of the product/system.

In considering that 75 % of those individuals who are in extreme poverty are rural farmers (The Mulago Foundation 2012), the ability to transport goods more efficiently would represent a potential means of increasing their income. In addition to these individuals, others could also benefit from the ability to obtain an inexpensive means of transporting goods and other cargo. With this motivation, the example presented in this section focuses on the identification of a modular plywood cart that is capable of adapting to various cargo types so as to meet a variety of user needs, while maintaining the lowest possible material costs.

Noting that increases in income will result in changes in what individuals view as affordable, preferences dictating the acceptable sales prices of carts for various cargo types/capacity will also change over time. In addition, the other sources of change for this example include the cart structure analysis models and concepts due to various load scenarios (i.e., operation environments). These load scenarios come from the identification of three different types of cargo. A description of these cargo types are provided below.

(1) *Stackable Cargo:* This cargo is characterized by objects that can be stacked or placed next to each other, and only require a tie-down (i.e., rope or other lashing) to secure the cargo onto the cart. Examples of this cargo type include bricks, buckets, barrels, boxes, etc.
(2) *Low Density Non-Stackable Cargo:* This cargo is characterized by objects that are low in density, and can only be stacked if there is a structural aspect of the cart to contain the cargo within the boundaries of the cart bed (sides). Examples of this cargo type include foam, straw, clothing, etc.
(3) *High Density Non-Stackable Cargo:* This cargo is characterized by objects that are high in density, and again require a structural aspect of the cart to contain the cargo within the boundaries of the cart bed. Examples of this cargo type include soil, gravel, fresh produce, etc.

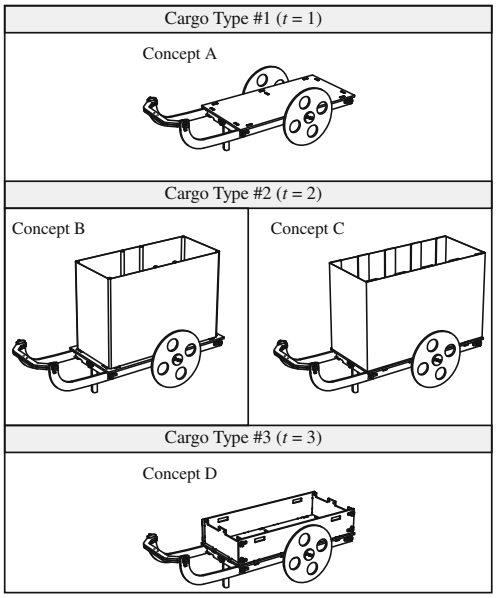

Fig. 6 CAD models of concept plywood cart designs for each cargo type

Figure 6 presents concept plywood cart designs providing the structural elements identified in the cargo type definitions. The time sequence that these concepts are assumed to be desired, based on the relative costs of the concepts, is also illustrated in the figure by the assignment of $t = 1, 2, 3$ to the stackable cargo (Concept A – Flatbed Cart), low density non-stackable cargo (Concept B – Poles w/Cloth Sides Cart, Concept C – Wood Slats w/Cloth Sides Cart), and high density non-stackable cargo (Concept D – Wood Sided Cart), respectively. Also, note that these represent *non-modular* cart concepts, and not a concept modular system.

4.2 Method implementation

With a knowledge of the various cargo types and cart concepts being considered, the results and information needed to implement the method presented in Section 3 are now provided.

Method Steps A & B: For this example the objectives being considered are to minimize the sales price (S) and to maximize the cart bed area or volumetric capacity (A and V respectively), depending on whether or not the concept has sides. In order to characterize the dynamic multiobjective design space, analysis models for each of the identified cart concepts are needed.

In addition to the models of S (sum of the material, machining, and distribution costs all increased by a uniform mark-up of 40 %) and A or V, stress models of the frame (two different loading conditions), axle, and side concepts are developed. The first frame loading condition (Fig. 7a)

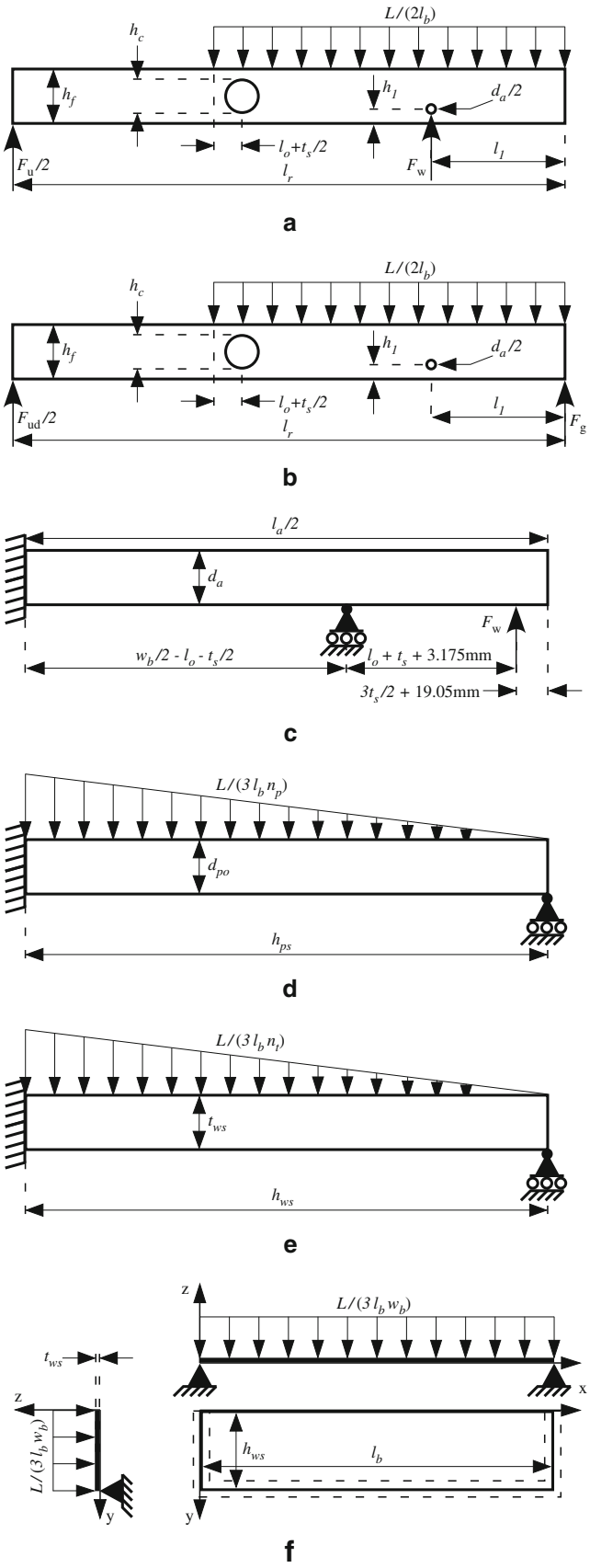

Fig. 7 **a** Cart frame loading for Concepts A-D. **b** Cart frame loading for dumping (only used by Concept D). **c** Axle loading for Concepts A-D. **d** Cart bed sides loading for Concept B. **e** Cart bed sides loading for Concept C. **f** Cart bed sides loading for Concept D

is applied to all concepts, assumes a maximum operational load (L) is uniformly distributed along the cart bed length (l_b), and is supported on the cart frame rails (long side members of the cart frame) by the reaction loads from the wheels (F_w) and cart operator (F_u). The second frame loading condition is only applied to Concept D, assumes the same distributed load, but is now supported by the operator and the end of the cart frame (See Fig. 7b) – simulates the operator lifting the front of the cart to dump out the load. For all of the concepts, the axle stress model looks at half of the axle (frame prevents the center deflection of the axle), and applies the wheel load from Fig. 7a as illustrated in Fig. 7c. For the three cart concepts with sides (Concepts B, C, and D), the assumed loads and boundary conditions used to determine the stress in the side structures are provided in Figs. 7d–f respectively.

It should be noted that for each concept, the frame is connected without metal fasteners, and the axle passes through the rails. As a result, the beams in Figs. 7a–b include stress concentrations in the form of circular holes to approximate the highest stress location cut-out for the implemented mortise and tenon joints (larger centered hole), and the axle (smaller non-centered hole). The formulas for both stress concentration factors come from Charts 4.88 and 4.89 of Pilkey and Pilkey (2008).

Definitions of the design objects (variables) shown in Fig. 7, and all other design objects pertaining to this example, are now provided:

l_r	Cart frame rail length (mm)
h_r	Overall height of the rails (mm)
l_o	Length of the bed overhanging the frame (mm)
l_s	Length of the plywood sheet (mm)
w_s	Width of the structure plywood sheet (mm)
t_s	Thickness of the structure plywood sheet (mm)
h_1	Axle center-height from the bottom edge of the rail (mm)
l_1	Axle center-distance from the rail end (mm)
d_a	Diameter of the axle (mm)
L	Maximum desired operational cart load (N)
l_b	Length of the cart bed (mm)
w_b	Width of the cart bed (mm)
h_c	Height of the mortise cut-out in the rails (mm)
h_f	Height of the cart frame beam members (mm)
F_u	Reaction force applied by the operator (N)
F_w	Reaction force applied by one wheel (N)
F_{ud}	Reaction force applied by the operator when dumping the cart load (N)

F_g Reaction force applied by the ground when dumping the cart load (N)
l_a Length of the axle (mm)
d_{po} Outer pole diameter for Concept B (mm)
d_{pi} Inner pole diameter for Concept B (mm)
h_{ps} Height of Concept B sides (mm)
n_p Number of poles used in Concept B (mm)
h_{ws} Height of Concept C and D sides (mm)
t_{ws} Sheet thickness of Concept C and D sides (mm)
n_t Number of tenons securing the Concept C sides
$L_{\text{fail}}^{(i)}$ Cart failure load (N)
LF Load multiplier for calculating $L_{\text{fail}}^{(i)}$
h_u Average waist height of the cart operator (mm)
d_w Diameter of the plywood cart wheels (mm)
d_t Diameter of the router tool (mm)
f_r Feed rate of the router (mm/s)
ϕ_{mach} Hourly machining rate ($/hr)
ϕ_a Axle material price ($/mm)
ϕ_{p} Material price for pole sides ($/mm)
ϕ_{ws} Material price for the wood sides ($/mm^2)
C_{bwnp} Cost of bolts, washers, nuts, and pins ($)
σ_f Maximum frame stress (MPa)
σ_a Maximum axle stress (MPa)
σ_{ps} Maximum stress in pole sides (MPa)
σ_{ws} Maximum stress wood sides (MPa)
θ Bed angle while transporting cargo (rad)
$\bar{g}_1$ Calculated difference between $l_b/2$ and l_1 (m)
$\bar{g}_2$ Calculated difference between l_r and l_b (m)
$\bar{g}_3$ Calculated clearance of the Concept D sides above the wheels (m)
$\bar{g}_4$ Calculated difference between l_s and l_r (m)
$\bar{g}_5$ Calculated left-over sheet width (m), assuming the rails/bed are cut as shown in Fig. 8

A summary of each concept's design objects for $t = \{1, 2, 3\}$, along with the corresponding values of $x_l^{(k^{(t)})}$, $x_u^{(k^{(t)})}$, and the diagonal entries in $w^{(k^{(t)})}$ needed to evaluate $(P1)$ are provided in Table 1. It should be noted that the bounds of the anticipated regions of interest as defined in Section 3.2 (Step B) are presented in Table 1 as the listed values of $S_l^{(k^{(t)})}$ and $S_u^{(k^{(t)})}$. In addition, for this example it is assumed the values of $y^{(k^{(t)})}$ have bounded uncertainties that result in the domain (h) of the uncertain parameters (c) being defined as $c_l^{(k^{(t)})} \leq c^{(k^{(t)})} \leq c_u^{(k^{(t)})}$. The values of $c_l^{(k^{(t)})}$ and $c_u^{(k^{(t)})}$ needed to evaluate $(P1)$ are also provided in Table 1.

Using MATLAB's fmincon function, the resulting dynamic s-Pareto frontier for the *non-modular* cart concepts shown in Fig. 6 at each time step within the identified region of interest is illustrated in Fig. 9. From Fig. 9, it can be seen that due to the changes in loading conditions, concepts, and required analysis models, the s-Pareto frontier does change.

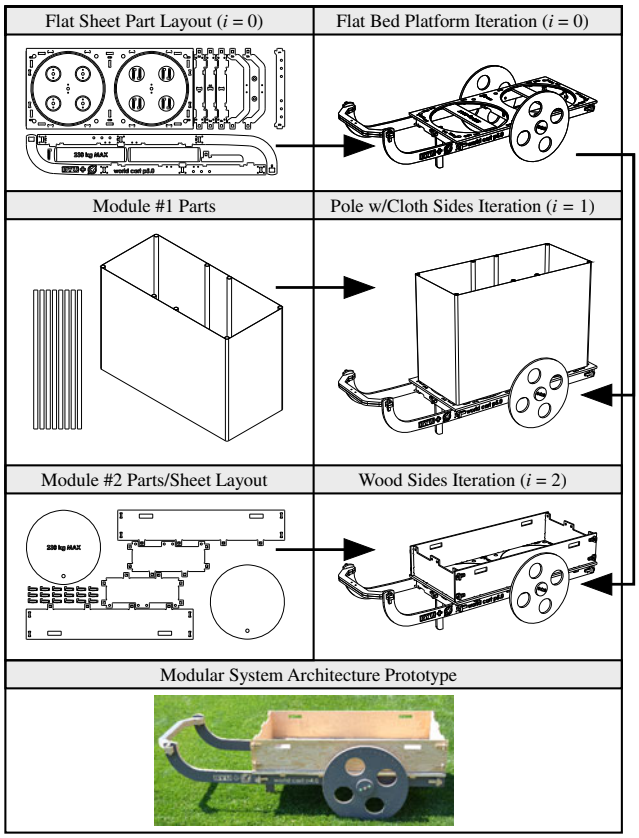

Fig. 8 Illustrations of the modular cart system concept iterations, the flat sheet part layouts for the platform and module #2, the module #1 parts, and a preliminary physical prototype that was field tested in Peru

In addition, it should also be observed that although Concepts B and C are considered for $t = 2$, Concept C does not contribute to the s-Pareto frontier for $t = 2$ because it is always dominated by Concept B in terms of the objectives for $t = 2$ to minimize the sales price (S) and maximize the volumetric cart capacity (V).

Method Steps C & D: In considering the differences between the concepts that comprise the dynamic s-Pareto frontier shown in Fig. 9, a slot modular architecture (Ulrich and Eppinger 2004) approach is selected for the modular cart development. The subsequent definitions of n_{m} and δ are as follows:

$$n_{\text{m}} = 2 \tag{28}$$

$$\delta = \begin{bmatrix} 1 & 1 \\ 1 & 2 \\ 1 & 3 \end{bmatrix} \tag{29}$$

Using this knowledge of the desired modular progression and architecture, the modular cart system concept is developed. In order to reduce the material and machining costs of the modular system, a structural topology was manually selected in which all structural elements of the platform cart design (flat bed cart) could be cut from a single sheet of

Table 1 Values of the design objects (x), uncertain parameter (c) domain limits, and the objective identifiers (diagonal entries in $w^{(k^{(t)})}$) needed to evaluate ($P1$) for the cart example

	$t=1$					$t=2$										$t=3$				
	$k=1$					$k=1$					$k=2$					$k=1$				
x (units)	w	x_l	x_u	c_l	c_u	w	x_l	x_u	c_l	c_u	w	x_l	x_u	c_l	c_u	w	x_l	x_u	c_l	c_u
d_a (mm)	0	19.05	19.05	−0.051	0	0	19.05	19.05	−0.051	0	0	19.05	19.05	−0.051	0	0	19.05	19.05	−0.051	0
l_b (mm)	0	1143	1625.6	−0.254	0.254	0	1143	1625.6	−0.254	0.254	0	1143	1625.6	−0.254	0.254	0	1143	1625.6	−0.254	0.254
w_b (mm)	0	609.6	812.8	−0.254	0.254	0	609.6	812.8	−0.254	0.254	0	609.6	812.8	−0.254	0.254	0	609.6	812.8	−0.254	0.254
h_f (mm)	0	95.25	107.95	−0.254	0.254	0	95.25	107.95	−0.254	0.254	0	95.25	107.95	−0.254	0.254	0	95.25	107.95	−0.254	0.254
l_1 (mm)	0	508	711.2	−0.254	0.254	0	508	711.2	−0.254	0.254	0	508	711.2	−0.254	0.254	0	508	711.2	−0.254	0.254
h_1 (mm)	0	25.4	34.9	−0.254	0.254	0	25.4	34.9	−0.254	0.254	0	25.4	34.9	−0.254	0.254	0	25.4	34.9	−0.254	0.254
t_s (mm)	0	19.05	28.58	−1.778	0	0	19.05	28.58	−1.778	0	0	19.05	28.58	−1.778	0	0	19.05	28.58	−1.778	0
w_s (mm)	0	1193.8	1193.8	−1.588	0	0	1193.8	1193.8	−1.588	0	0	1193.8	1193.8	−1.588	0	0	1193.8	1193.8	−1.588	0
l_s (mm)	0	2438.4	2438.4	−1.588	0	0	2438.4	2438.4	−1.588	0	0	2438.4	2438.4	−1.588	0	0	2438.4	2438.4	−1.588	0
l_o (mm)	0	38.1	38.1	0	0	0	38.1	38.1	0	0	0	38.1	38.1	0	0	0	38.1	38.1	0	0
d_t (mm)	0	9.525	9.525	0	0	0	9.525	9.525	0	0	0	9.525	9.525	0	0	0	9.525	9.525	0	0
f_r (mm/s)	0	50.8	50.8	0	0	0	50.8	50.8	0	0	0	50.8	50.8	0	0	0	50.8	50.8	0	0
L (N)	0	2224.1	2224.1	0	0	0	2224.1	2224.1	0	0	0	2224.1	2224.1	0	0	0	2224.1	2224.1	0	0
LF	0	2	100	0	0	0	2	100	0	0	0	2	100	0	0	0	2	100	0	0
h_c (mm)	0	47.625	53.975	−0.255	0.254	0	47.625	53.975	−0.255	0.254	0	47.625	53.975	−0.255	0.254	0	47.625	53.975	−0.255	0.254
h_u (mm)	0	889	889	0	0	0	889	889	0	0	0	889	889	0	0	0	889	889	0	0
ϕ_{mach} ($/hr)	0	20	20	0	0	0	20	20	0	0	0	20	20	0	0	0	20	20	0	0
ϕ_a ($/m)	0	4.10	4.10	0	0	0	4.10	4.10	0	0	0	4.10	4.10	0	0	0	4.10	4.10	0	0
C_{bwnp} ($)	0	2	2	0	0	0	2	2	0	0	0	2	2	0	0	0	2	2	0	0
l_r (mm)	0	1828.8	2333.6	−0.255	0.254	0	1828.8	2333.6	−0.255	0.254	0	1828.8	2333.6	−0.255	0.254	0	1828.8	2333.6	−0.255	0.254
h_r (mm)	0	254	574.7	−0.255	0.254	0	254	574.7	−0.255	0.254	0	254	574.7	−0.255	0.254	0	254	574.7	−0.255	0.254
d_w (mm)	0	508	762	−0.255	0.254	0	508	762	−0.255	0.254	0	508	762	−0.255	0.254	0	508	762	−0.255	0.254
h_{ps} (mm)	–	–	–	–	–	0	1219.2	1828.8	−0.255	0.254	–	–	–	–	–	–	–	–	–	–
n_p	–	–	–	–	–	0	8	8	0	0	–	–	–	–	–	–	–	–	–	–
d_{po} (mm)	–	–	–	–	–	0	33.4	33.4	−0.127	0.127	–	–	–	–	–	–	–	–	–	–
d_{pi} (mm)	–	–	–	–	–	0	26.24	26.24	−0.127	0.127	–	–	–	–	–	–	–	–	–	–
ϕ_{p} ($/m)	–	–	–	–	–	0	2.38	2.38	0	0	–	–	–	–	–	–	–	–	–	–
h_{ws} (mm)	–	–	–	–	–	–	–	–	–	–	0	254	939.8	−0.254	0.254	0	302.2	304.8	−0.254	0.254
n_t (mm)	–	–	–	–	–	–	–	–	–	–	0	8	8	0	0	–	–	–	–	–
t_{ws} (mm)	–	–	–	–	–	–	–	–	–	–	0	12.7	12.7	−0.178	0	0	12.7	12.7	−0.178	0
w_{st} (mm)	–	–	–	–	–	–	–	–	–	–	0	38.1	50.8	−0.254	0.254	0	38.1	50.8	−0.254	0.254
ϕ_{ws} ($/m^2)	–	–	–	–	–	–	–	–	–	–	0	30	30	0	0	0	30	30	0	0
S ($)	1	60	105	–	–	1	95	153	–	–	1	95	153	–	–	1	112	154	–	–

Table 1 (continued)

	$t=1$				$t=2$				$t=3$			
	$k=1$				$k=1$		$k=2$		$k=1$			
A (m^2)	−1	0.697	1.333	–	–	–	–	–	–	–	–	–
V (m^3)	–	–	–	–	−1	1.147	2.327	–	–	−1	0.229	0.557
L_{fail} (N)	0	4448.2	22241	–	0	4448.2	22241	–	–	0	4448.2	22241
σ_f (MPa)	0	0	76.532	–	0	0	76.532	–	–	0	0	76.532
σ_a (MPa)	0	0	344.7	–	0	0	344.7	–	–	0	0	344.7
σ_{ps} (MPa)	–	–	–	–	0	0	99.63	–	–	–	–	–
σ_{ws} (MPa)	–	–	–	–	–	–	–	0	0	0	0	76.532
θ (rad)	0	0	0.297	–	0	0	0.297	0	0	0	0	0.297
F_u (N)	0	0	444.8	–	0	0	444.8	0	0	0	0	444.8
F_{ud} (N)	–	–	–	–	–	–	–	–	–	0	0	2224.1
$\bar{g}_1$ (m)	0	0	∞	–	0	0	∞	0	0	0	0	∞
$\bar{g}_2$ (m)	–	–	–	–	–	–	–	–	–	0	0	∞
$\bar{g}_3$ (m)	0	0.686	0.762	–	0	0.686	0.762	0	0.762	0	0.686	0.762
$\bar{g}_4$ (m)	0	0	∞	–	0	0	∞	0	∞	0	0	∞
$\bar{g}_5$ (m)	0	0	∞	–	0	0	∞	0	∞	0	0	∞

19.05 mm or 28.58 mm plywood. The flat sheet part layout of this concept, including the necessary interface features for pole and box sides is illustrated in Fig. 8. Also shown in Fig. 8 are images of the CAD models of the assembled system iterations, the two modules (pole w/cloth and box side), and a picture of a preliminary physical prototype that was built and field tested in Peru (prototype created with 28.58 mm plywood). It should be noted that the purpose of this field testing was to validate the bounds of the regions of interest and the uncertain area of the regions of interest illustrated in Fig. 9. As such, since the purpose of this first prototype was to illustrate the design concept to the target group in Peru, the design of the illustrated prototype was set by the authors intuition without the use of numerical optimization.

Method Step E: In order to facilitate the modular system identification, the limits of the modular-system design objects ($\hat{x}_{u/l}$), the corresponding diagonal entries in $\hat{w}$, and the domain limit vectors of the modular-system uncertain parameters ($\hat{c}_{u/l}$) needed to evaluate (*P2*) are provided in Table 2. The bounds of the uncertain areas of the regions of interest ($\hat{S}^{(i)}_{u/l,\text{unc}}$) needed to evaluate (*P2*) are also provided in Table 2.

Optimization of the modular system is also performed using MATLAB's fmincon function, with the modular cart system design being directly selected using a weighted-sum aggregate objective function ($w_J = \{0.5, 1, 1\}$, $\hat{C} = \{\hat{A}^{(0)}, \hat{V}^{(1)}, \hat{V}^{(2)}\}$,$w_{\hat{C}} = 1.5$). The aggregate objective function and penalty function ($\hat{\Lambda}$) definitions used to evaluate (*P2*) are provided below:

$$\hat{\Lambda}^{(i)} = \begin{cases} 1 - \left(\frac{\hat{V}^{(i)} - \hat{\mu}^{(i)}_{u,\text{unc}}}{\hat{V}^{(i)}_u - \hat{\mu}^{(i)}_{u,\text{unc}}} + 1 \right)^{-1} & , \hat{V}^{(i)} > \hat{\mu}^{(i)}_{u,\text{unc}} \\ 1 - \left(\frac{\hat{\mu}^{(i)}_{l,\text{unc}} - \hat{V}^{(i)}}{\hat{\mu}^{(i)}_{l,\text{unc}} - \hat{V}^{(i)}_l} + 1 \right)^{-1} & , \hat{V}^{(i)} > \hat{\mu}^{(i)}_{l,\text{unc}} \\ 0 & , \text{else} \end{cases} \tag{30}$$

$$J = \sum_{i=0}^{n\text{m}} \left(w^{(i)}_J \cdot (\hat{\Theta}^{(i)} + \hat{\Lambda}^{(i)}) - w_{\hat{C}} \cdot \hat{C}^{(i)} \right) \tag{31}$$

Figure 9 presents the objective space results for the optimized modular cart system and preliminary prototype. Although both systems are within the identified regions of interest, the prototype system has an average $\hat{\Theta}$ and $\hat{\Lambda}$ of 0.57 and 0.33, while the optimized system has averages of 0.04 and 0 respectively – represents ∼93 % and 100 % respective improvements. Figure 10 provides images of a physical prototype implementing the optimization results.

5 Concluding remarks

In response to the limitations of a six-step modular-system optimization method developed by the authors (Lewis and

Table 2 Limit values of the modular-system design objects ($\hat{x}_{u/l}$), uncertain parameter domain limits ($\hat{c}_{u/l}$), and the corresponding diagonal entries in $\hat{w}^{(i)}$ needed to evaluate (*P2*)

$\hat{x}$	$\hat{w}^{(0)}$	$\hat{w}^{(1)}$	$\hat{w}^{(2)}$	x_l	x_u	c_l	c_u
$\hat{d}_a$	0	0	0	19.05	19.05	−0.051	0
$\hat{l}_b$	0	0	0	1143	1625.6	−0.254	0.254
$\hat{w}_b$	0	0	0	609.6	812.8	−0.254	0.254
$\hat{h}_f$	0	0	0	95.25	107.95	−0.254	0.254
$\hat{l}_1$	0	0	0	508	711.2	−0.254	0.254
$\hat{h}_1$	0	0	0	25.4	34.9	−0.254	0.254
$\hat{t}_s$	0	0	0	19.05	28.58	−1.778	0
$\hat{w}_s$	0	0	0	1193.8	1193.8	−1.588	0
$\hat{l}_s$	0	0	0	2438.4	2438.4	−1.588	0
$\hat{l}_o$	0	0	0	38.1	38.1	0	0
$\hat{d}_t$	0	0	0	9.525	9.525	0	0
$\hat{f}_r$	0	0	0	50.8	50.8	0	0
$\hat{L}$	0	0	0	2224.1	2224.1	0	0
$\hat{LF}$	0	0	0	2	100	0	0
$\hat{h}_c$	0	0	0	47.625	53.975	−0.255	0.254
$\hat{h}_u$	0	0	0	889	889	0	0
$\hat{\phi}_{\text{mach}}$	0	0	0	20	20	0	0
$\hat{\phi}_a$	0	0	0	4.10	4.10	0	0
$\hat{C}_{\text{bwnp}}$	0	0	0	2	2	0	0
$\hat{l}_r$	0	0	0	1828.8	2333.6	−0.255	0.254
$\hat{h}_r$	0	0	0	254	574.7	−0.255	0.254
$\hat{d}_w$	0	0	0	508	762	−0.255	0.254
$\hat{h}_{ps}$	–	0	–	1219.2	1828.8	−0.255	0.254
$\hat{n}_p$	–	0	–	8	8	0	0
$\hat{d}_{po}$	–	0	–	33.4	33.4	−0.127	0.127
$\hat{d}_{pi}$	–	0	–	26.24	26.24	−0.127	0.127
$\hat{\phi}_{\text{p}}$	–	0	–	2.38	2.38	0	0
$\hat{h}_{ws}$	–	–	0	302.2	304.8	−0.254	0.254
$\hat{t}_{ws}$	–	–	0	12.7	12.7	−0.178	0
$\hat{\phi}_{\text{ws}}$	–	–	0	30	30	0	0
$\hat{S}^{(0)}$	1	–	–	60	105	–	–
$\hat{A}^{(0)}$	−1	–	–	0.697	1.333	–	–
$\hat{L}^{(i)}_{\text{fail}}$	0	0	0	4448.2	22241	–	–
$\hat{\sigma}^{(i)}_f$	0	–	0	0	76.532	–	–
$\hat{\sigma}_a$	0	–	–	0	344.7	–	–
$\hat{\theta}$	0	–	–	0	0.297	–	–
$\hat{F}_u$	0	–	–	0	444.8	–	–
$\hat{\bar{g}}_1$	0	–	–	0	∞	–	–
$\hat{\bar{g}}_2$	–	–	0	0	∞	–	–
$\hat{\bar{g}}_3$	0	–	–	0.686	0.762	–	–
$\hat{\bar{g}}_4$	0	–	–	0	∞	–	–
$\hat{\bar{g}}_5$	0	–	–	0	∞	–	–
$\hat{S}^{(1)}$	–	1	–	95	153	–	–
$\hat{V}^{(1)}$	–	−1	–	1.147	2.327	–	–
$\hat{\sigma}_{ps}$	–	0	–	0	99.63	–	–
$\hat{S}^{(2)}$	–	–	1	112	154	–	–
$\hat{V}^{(2)}$	–	–	−1	0.229	0.557	–	–
$\hat{\sigma}_{ws}$	–	–	0	0	76.532	–	–
$\hat{F}_{ud}$	–	–	0	0	2224.1	–	–
$\hat{\bar{g}}_6$	–	–	0	0	0	–	–
$\hat{\bar{g}}_7$	–	–	0	0	∞	–	–

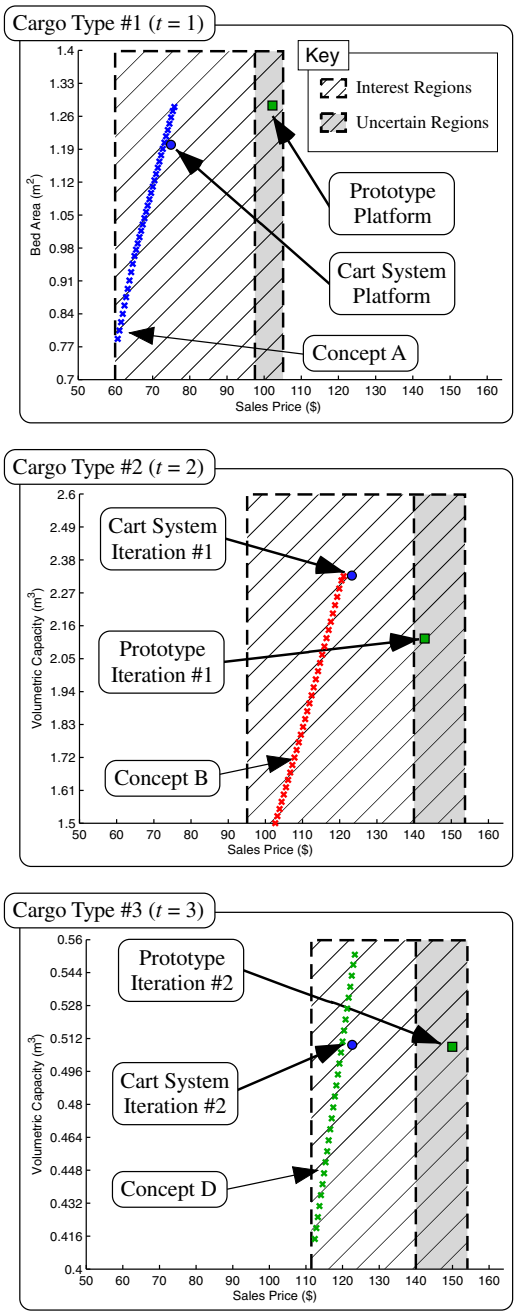

Fig. 9 Representation of the s-pareto frontier obtained for each time-step (cargo type), along with the performance of each iteration of both the preliminary prototype in Fig. 8 and the optimized modular cart system

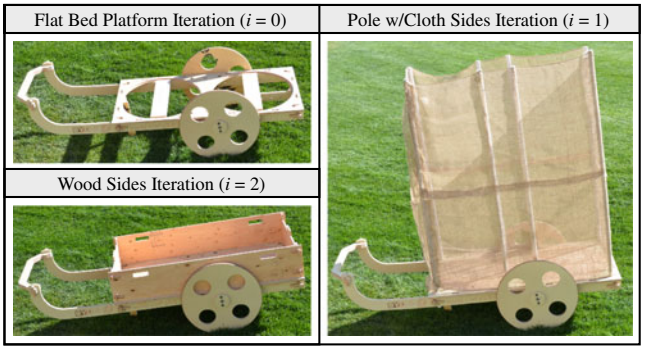

Fig. 10 Images of a physical prototype created with 19.05 mm plywood implementing the modular cart system optimization results represented in Fig. 9

Mattson 2012), an improved five-step method that builds on recent developments in multiobjective problem formulations of dynamic s-Pareto frontiers was presented. Notable improvements to the method include: (i) the added ability to allow for changes in system concepts and analysis models at different time-steps, and (ii) the inclusion of provisions for incorporating uncertainty analysis. The presented method provides a quick and efficient framework to explore the design space at each known time-step, and leverages the entire dynamic s-Pareto frontier within identified regions of interest at each time-step to guide the development and identification of a modular system design. Application of the presented method was illustrated through the identification of a modular plywood cart for developing countries capable of adapting to three different cargo types.

The usefulness of the presented method can be observed through the comparison of the modular cart system performance in terms of the Pareto offset ($\hat{\Theta}$), and the uncertain region of interest penalty ($\hat{\Lambda}$) for the different iterations of a preliminary prototype and the optimized modular system. By incorporating within the method the ability to identify the dynamic s-Pareto Frontier (allow for changes in system concepts/analysis models) and account for uncertainty, the optimization of the modular-system was improved by reducing the average $\hat{\Theta}$ and $\hat{\Lambda}$ by ~93 % and 100 % respectively compared to the preliminary prototype. In addition, recognizing the importance of cost in developing products for those in extreme poverty ($30 ≈ 1 months income), the optimized modular cart respectively reduced the overall price of the three system iterations by $27.31 (~27 %), $19.60 (~14 %), and $27.33 (~18 %) compared to the preliminary prototype design.

In considering the use of the presented method, it should be noted that the method is limited to applications where the design concepts, analysis models, use environments, and/or design selection preferences can be predicted with reasonable accuracy. As such, in fast paced industries where new technologies or materials are developed quickly, the presented method does have limitations. However, if the improvements in technologies/materials can be predicted with some indication of the uncertainty in that prediction, then the method could be used to help designers/engineers to look beyond the current product/iteration to make better decisions in the present. Specifically, early stage platforms

and modules could be designed to better interface with new technologies before they are fully developed.

Acknowledgments We would like to recognize the National Science Foundation Grant CMMI-0954580 and our design colleagues at Rocketship, Inc. for funding this research.

References

Box GE, Tiao GC (1992) Bayesian inference in statistical analysis. Wiley, Hoboken, NJ, ISBN: 9780471574286

Chen W, Wassenaar HJ (2001) An approach to decision-based design. In: Proceedings of DETC'01, ASME 2001 design engineering technical conference and computers and information in engineering conference, Pittsburgh, Penn., DETC2001/DMT-21683

Chen W, Wiecek MM, Zhang J (1999) Quality utility - a compromise programming approach to robust design. ASME J Mech Des:121

Chen W, Sahai A, Messac A, Sundaraj GJ (2000) Exploring the effectiveness of physical programming in robust design. ASME J Mech Des 122(2):155–163

Das I (1999) A preference ordering among various pareto optimal alternatives. Struct Multidiscip Optim 18(1):30–35

DeVor RE, Chang TH, Sutherland JW (1992) Statistical quality design and control: contemporary concepts and methods. Prentice Hall, New Jersey, pp 525–535

Evans JW, Zawadzki RJ, Jones SM, Olivier SS, Werner JS (2009) Error budget analysis for an adaptive optics optical coherence tomography system. Opt Express 17(16):13,768–13,784

Fisher M (2006) Income is development. Innovations Journal Winter 2006:9–30

Frangopol DM, Corotis RB (1996) Reliability-based structural system optimization: State-of-the-art verses state-of-the-practice. In: Proceedings of the twelfth conference on analysis and computation, pp 67–78

Frischknecht BD, Peters DL, Papalambros PY (2011) Pareto set analysis: local measures of objective coupling in multiobjective design optimization. Struct Multidiscip Optim 43(5):617–630. doi:10.1007/s00158-010-0599-2

Glancy C (1999) A second-order method for assembly tolerance analysis. In: Proceedings of the 1999 ASME design engineering technical conferences, DAC-8707 in DETC99

Gurav SP, Goosen JFL, vanKeulen F (2005) Bounded-but-unknown uncertainty optimization using design sensitivities and parallel computing: Application to mems. Struct Optim Comput Mech 83(14):1134–1149. doi:10.1016/j.compstruc.2004.11.021

Gurnani AP, Lewis K (2008) Using bounded rationality to improve decentralized design. AIAA J 46(12):3049–3059. doi:10.2514/135776

Halton JH (1960) On the efficiency of certain quasi-random sequences of points in evaluating multi-dimensional integrals. Numerische Mathematik 2:84–90. doi:10.1007/BF01386213

Hamaker HC (1995) Improved estimates of the range of errors on photomasks using measured values of skewness and kurtosis. In: Proceedings of SPIE 2621(198(1995))

Hammersley JM (1960) Monte carlo methods for solving multivariate problems. Ann N Y Acad Sci 86:844–874

Hayes B (2003) A lucid interval. Am Sci 91(6):484–488

Hutcheson RS, McAdams DA (2010) A hybrid sensitivity analysis for use in early design. J Mech Des 132(11):111,007

Jackson PS (1982) A second-order moments method for uncertainty analysis. IEEE Trans Reliab R-31(4):382–384

Johnson NG, Hallam A, Bryden M, Conway S (2006) Sustainable and market-based analysis of cooking technologies in developing countries. In: Proceeding of the ASME international mechanical engineering congress and exposition, IMECE2006-15375

Kasprzak EM, Lewis KE (2000) An approach to facilitate decision tradeoffs in pareto solution sets. Engineering Valuation and Cost Analysis 3:173–187

Koch PN (2002) Probabilistic design: optimizing for six sigma quality. In: 43rd AIAA/ASME/ASCE/AHS structures, structural dynamics, and materials conference, AIAA–2002–1471

Larson B, Anderson TV, Mattson CA (2010) System behavioral model verification for concurrent design modeling. In: 13th AIAA/ISSMO Multidiscip Anal Optim Conf, AIAA-2010-9104

Lewis PK, Mattson CA (2012) A method for developing systems that traverse the pareto frontiers of multiple system concepts through modularity. Struct Multidiscip Optim 45(4):467–478. doi:10.1007/s00158-011-0735-7

Lewis PK, Murray VR, Mattson CA (2011) A design optimization strategy for creating devices that traverse the Pareto frontier over time. Struct Multidiscip Optim 43(2):191–204. doi:10.1007/s00158-010-0555-1

Lewis PK, Tackett M, Mattson CA (2012) Considering dynamic pareto frontiers in decision making. In: 8th AIAA Multidiscipl Des Optim Specialist Conf, Honolulu, Hawaii, AIAA-2012-1849

Li G, Zhang K (2011) A combined reliability analysis approach with dimension reduction method and maximum entropy method. Struct Multidiscipl Optim 43(1):121–134. doi:10.1007/s00158-010-0546-2

Lombardi M, Haftka RT (1998) Anti-optimization technique for structural design under load uncertainties. Comp Methods Appl Mech Eng 157(1–2):19–31

Mattson CA, Messac A (2003) Concept selection using s-pareto frontiers. AIAA J 41(6):1190–1204

Melchers RE (1999) Structural reliability: analysis and prediction. Ellis Horwood Series in Civil Engineering. Wiley, New York

Messac A, Ismail-Yahaya A (2002) Multiobjective robust design using physical programming. Struct Multidiscip Optim 23(5):357–371

Messac A, Mattson CA (2004) Normal constraint metthod with guarentee of even representation of complete pareto frontier. AIAA J 42(10):2101–2111

Owen AB (1998) Latin supercube sampling for very high-dimensional simulations. ACM Trans Model Comput Simul 86(1):71–102

Parkinson A, Sorensen C, Pourhassan N (1995) A general approach for robust optimal design. ASME J Mech Des 115:74–80

Pilkey WD, Pilkey DF (2008) Peterson's stress concentration factors, 3rd edn. Wiley, New York

Polak P (2005) The big potential of small farms. Sci Am 293(3)

Strong MB, Magleby SP, Parkinson AR (2003) A classification method to compare modular product concepts. In: The ASME 2003 Design Engineering Technical Conferences

Su J, Renaud JE (1997) Automatic differentiation in robust optimization. AIAA J 35(6):1072–1079

Taguchi G (1993) Taguchi on robust technology development: bringing quality engineering upstream. ASME Press, New York

Thanedar PB, Kodiyalam S (1991) Structural optimization using probabilistic constraints. In: AIAA/ASME/ASCE/AHS Structures, Structural Dynamics, and Materials Conference, AIAA-91-0922-CP

The Mulago Foundation (2012) One acre fund: Planting prosperity. http://www.mulagofoundation.org/portfolio/one-acre-fund

Todoroki A, Sekishiro M (2008) Modified efficient global optimization for a hat-stiffened composite panel with buckling constraint. AIAA J 46(9):2257–2264. doi:10.2514/134548

Ulrich K, Eppinger S (2004) Product Design and Development, 4th edn. McGraw-Hill

Vardeman SB (1994) Statistics for engineering problem solving. PWS Publishing Company, Boston, MA. ISBN: 0-534-92871-4

World Resources Institute and International Finance Corporation (2007) The next 4 billion: market size and business strategy at the base of the pyramid. World Bank, Tech Rep. http://rru.worldbank.org/thenext4billion

Xiong F, Guo K, Zhou W (2011) Uncertainty propagation techniques in probabilistic design of multilevel systems. In: 2011 International conference on quality, reliability, risk, maintenance, and safety Engineering, pp 874–878